Journal of Composites and Compounds 7(2025) 1-4

Available Online at www.jourcc.com

Journal homepage: www.JOURCC.com

Journal of Composites and Compounds

Effect of carbon nanotubes on morphology and mechanical properties of nickel/graphene oxide coating on copper substrates

Mahdi Aghaee Malayeri*, Hassan Koohestani, Mohammad Tajally

Faculty of Materials and Metallurgical Engineering, Semnan University, Semnan, Iran

ABSTRACT

A novel nickel-graphene oxide/carbon nanotube (Ni/GO/CNT) composite coating was deposited on a copper substrate via the electrodeposition method with different Concentration of CNT (0.5, 1 and 1.5 g/L). In this paper, the effect of CNT addition on the mechanical properties and morphology was investigated. For phase analysis, X-ray diffraction was performed, but the peak related to GO was not identified. Raman results confirm the presence of GO and CNT in Ni/GO/CNT coatings. The composite coatings with 1 g/L of CNT exhibited the maximum hardness, with a value of 840 HV. Furthermore, Ni/G0.5O/1CNT coating showed excellent adhesion strength, and minimum wear loss (0.0002 g). However, further addition CNT to 15 g/L led to a decrease in hardness. This is attributed to the agglomeration of CNT, which weakens the integrity of the structure.

Peer review under responsibility of UGPH.

ARTICLE INFORMATION

Article History:
Received 13 October 2025
Received in revised form 27 November 2025
Accepted 14 December 2025

Keywords:
Graphene oxide
Agglomeration
Carbon nanotube
Hardness
Weight loss

1. Introduction

Researchers have suggested the use of surface modification to increase the efficiency and service life of copper sheets, due to the damage caused by the use of copper pipes during steel casting operations, such as wear of the outlet area and erosion due to thermal stress, the use of copper surface modification is required [1-3]. Nickel-Graphene coating is one of the most widely used surface modifications for copper [4, 5]. Studies by Chen et al. [6] show that the nickel -graphene oxide (GO) coating reduces the friction coefficient and wear rate. Algol et al. [7] investigated the effect of graphene concentration on the tribological behavior of nickel-graphene coatings. They found that tribological properties increased with increasing GO concentration. However, GO sheets are prone to agglomeration due to strong van der Waals forces and high surface area, which degrades the coating's properties. This phenomenon becomes more apparent when higher concentrations of GO are required [8-10]. To overcome these limitations, incorporating of one-dimensional (1D) carbon nanotubes (CNT) with GO sheets is a promising way to improve the properties of composite coatings [11, 12]. CNTs are of interest not only in biological and medical applications, but also for electrical and mechanical applications due to their significant advantages such as chemical stability, remarkable mechanical strength and high elastic modulus [13-15]. CNT can act as a spacer between GO sheets to prevent them from agglomerating. Concurrently, graphene sheets connect CNT by creating a bridging mechanism. CNT also enhance charge transfer by bridging between nickel particles [16]. Dong et al. [17] studied the effect of CNT on tribological properties and microstructure of Ni/GO/CNT using ultrasonic-assisted electrodeposition. They found that with the addition of CNT concentration, the microhardness increased compared to Ni pure. Therefore, it is believed that the use of CNT reinforcements is ideal in the production of high-performance composite coatings. In this study, the mechanical properties, including hardness and wear behavior, of ternary Ni/GO/CNT coatings with different concentrations of CNT (0.5, 1, 1.5 g/L) were investigated. It has been shown that CNT can be successfully incorporated between Ni and GO in the coatings.

2. Materials and methods

2.1. Materials

Nickel sulfate ($NiSO_4.6H_2O$, Purity: 98.6) and nickel chloride ($NiCl_2.6H2O$, Purity: 98.2%) were provided from Umicore Co (Ltd., Belgium). Nickel sheet and GO colloidal solution (size 1 nm and concentration 1 g/L) were provided from Falcon Co (99.97 wt%, Norway) and Pars Nanomaterials Co (Tehran, Iran), respectively. Boric acid (H_3BO_3, Purity: 99.8%) and sodium dodecyl sulfate (SDS, Purity: 95.8%) were purchased from Merck Co (Ltd., Germany). A copper sheet was cut to 50 × 50 × 2 mm pieces. The sample surfaces were mechanically polished using 80

* *Corresponding author: Mahdi Aghaee Malayeri, Email: mahdiaghaee@semnan.ac.ir*

https://doi.org/10.61882/jcc.7.4.5

to 2000 SiC grinding papers. Then, Samples were dipped in a solution containing 200 ml of distilled water and 20 ml of 96% sulfuric acid for 40 seconds to remove surface oxides. After that, the Samples were subsequently degreased ultrasonically (Power 200w, time: 35 min) in acetone to eliminate any organic contaminants.

2.2. Method

Table 1 shows the compositions of the bath and the electrodeposition process parameters. The bath temperature was maintained at 35 °C, and the solution was stirred continuously using a magnetic stirrer at a constant speed of 300 rpm. The pH of the bath was set to an acidic range of 4 to 5. The electrodeposition was performed in a standard two-electrode cell. The pre-treated copper sheet served as the cathode, while a pure Ni sheet acted as the anode. The electrodes were positioned parallel to each other at a distance of approximately 5 cm. A direct current (DC) power supply was used to apply a constant voltage of 1.8 V, which resulted in a current of 0.23 A. The coating time was fixed at 60 minutes for all experiments.

Table 1
The value of each in electrolyte of various composite coating.

Composition	Ni/0.5GO/ 0.5CNT	Ni/0.5GO/ 1CNT	Ni/0.5GO/ 1.5CNT
Nickel Sulfate (g/L)	56	56	56
Nickel Chloride (g/L)	10	10	10
Boric Acid (g/L)	8	8	8
Sodium Dodecyl Sulfate (g/L)	3	3	3
Graphene oxide (g/L)	0.5	0.5	0.5
Carbon Nanotubes (g/L)	0.5	1	1.5

2.3. Characterization

The identification of the phase compounds present in the coatings was carried out by X-ray diffraction. X-ray diffraction device (Bruker model D8 Advance, Germany). Field emission scanning electron microscopy (FESEM, MIRA3TESCAN model, Czech Republic) to investigate the surface morphology of the composite coatings. Raman spectroscopy (Model Takram SRM, Co. Teksan, Iran) was used to investigate chemical bonding and the presence of carbon elements. To evaluate the hardness of the coatings, a micro-hardness (MMT-7, Buehler model, Germany) was used under a load of 25 g for 10 seconds. To determine the wear resistance and to study tribological behavior of the coating, a pin-on-disk tester (CDT2S model, Iran) was used with a 52,100-steel pin with a diameter of 5 mm. Adhesion strength was performed to examine the adhesion of the composite coating to the substrate by adhesion tester (PosiTest AT-M Manual, Co. Defelsko).

3. Results and discussion

3.1. Phase and structural analysis

Fig. 1 presents the XRD patterns for the Ni/GO/CNT composite coatings deposited on a copper substrate. During electroplating, the GO is typically reduced to reduced graphene oxide (rGO). However, no characteristic peaks for GO or CNT were observed in the XRD patterns, which is attributed to their low concentration in the coatings. This difficulty in detecting the GO/CNT peak is consistent with previous reports in similar studies [8]. The most intense peaks are located at 2θ values of approximately 43.5°, 50.4°, and 74.1°, corresponding to the (111), (200), and (220) planes of the face-centered cubic (fcc) copper substrate (JCPDS card no. 04-0836). As seen, Ni peaks of the (111), (200), and (220) planes are observable at 44.75°, 52.1° and 76.6° angles. The intensity of Ni peaks increases with CNT concentration, which is likely attributable to the decrease in Ni deposition rate caused by the poor conductivity of GO. The crystal size of Ni particles was measured using the Scherr equation. The grain size of Ni particles in the coating Ni/0.5GO/0.5CNT, Ni/0.5GO/1CNT and Ni/0.5GO/1.5CNT was 40, 35 and 42 nm, respectively.

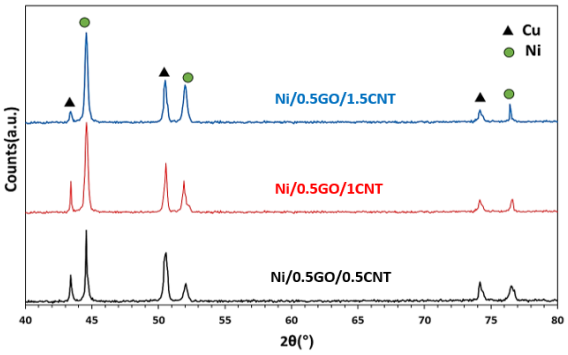

Fig. 1. XRD pattern of Ni/GO/CNT coating fabricated by electroplating process.

Raman spectroscopy confirmed the successful incorporation of GO and CNT within the composite coatings (Fig. 2). The spectrum exhibits characteristic carbon bands: a D band at 1338 cm^{-1}, corresponding to structural defects and disorder in the graphitic lattice, and a G band at approximately 1589 cm^{-1}, which is indicative of sp^2-hybridized carbon [18]. The intensity ratio of these bands (ID/IG) serves as a metric for the defect density within the carbon structures. As observed, the intensities of both the D and G peaks were enhanced with increasing CNT concentration, confirming a greater presence of carbonaceous reinforcement in the coating.

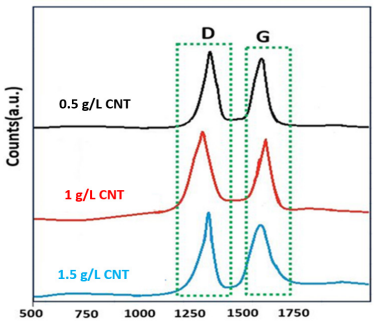

Fig. 2. Raman spectra of Ni/GO/CNT composite coatings.

The microstructure of Ni/GO/CNT composite coatings containing different amounts of CNT is shown in Fig. 3. The addition of CNT causes Ni particles to form heterogeneous nuclei on the CNT during the deposition process, which leads to increased Ni deposition, as reported by Dong et al. [17]. In the Ni/GO/CNT composite coating, Ni particles tend to deposit on the CNT. As the CNT concentration increases, Ni particles tend to precipitate on them. Furthermore, this process changes the morphology of Ni particles, promoting spherical growth instead of conical at the nucleation sites. The presence of CNT, due to their skeletal role, causes the size of Ni particles to decrease, as noted in the X-ray diffraction results. Moreover, CNT can enhance mechanical and tribological properties by bridging between GO sheets and Ni

particles. However, at higher CNT concentration (≥ 1.5 g/L), their incorporation with the Ni and GO matrix is limited, leading to agglomeration of carbon compounds (Fig. 3(E, F)).

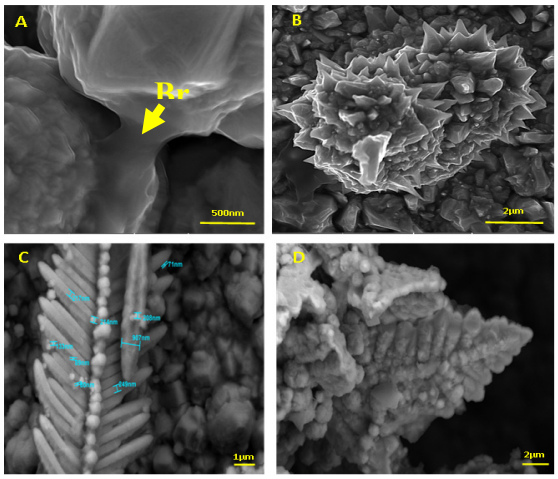

Fig. 3. FE-SEM micrograph of (A, B) Ni/0.5GO/0.5CNT, (C, D) Ni/0.5GO/1CNT, (E, F) Ni/0.5GO/1.5CNT at different magnification.

According to Fig. 4(A), in the composite coating, GO sheets act as bridging agents between Ni grains. Instead of forming a smooth and continuous layer on GO sheets, Ni particles nucleate spherically on the one-dimensional CNT structures with a high aspect ratio in a uniformly and densely. In Fig. 4(B), the co-deposition of GO sheets and CNT results in the production of a porous and spherical structure known as a 'cauliflower' structure, as described by Rao [19]. According to this model, the morphology results from two key processes: the lateral impingement and restricted growth of initial nuclei, and the formation of an ion-depleted diffusion layer. This depletion zone, caused by the consumption of soluble ions during reduction, leads to a decreased deposition rate that ultimately self-limits growth and defines the final topography. On the other hand, the presence of CNT prevents the cauliflower clusters from connecting to each other. The nanotubes intertwine with the growing GO sheets and nickel particles, acting as a reinforcing scaffold or bridge. In Fig. 4(C-D) reveals the branched nature of CNT, where Ni nanoparticles grow on the CNT, as reported previously in similar studies.

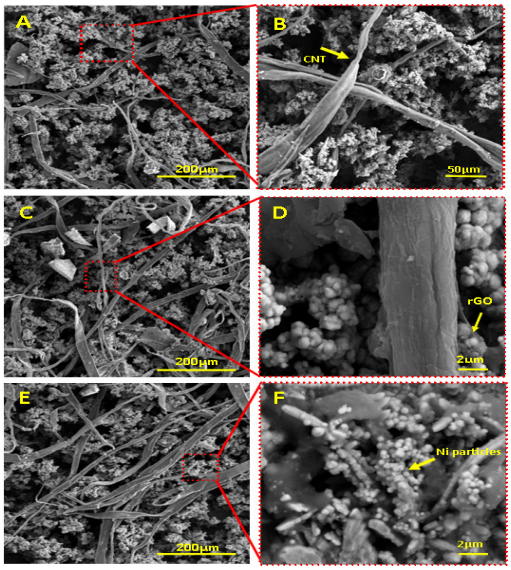

Fig. 4. FE-SEM images of Ni/GO/CNT composite showing (A) GO sheets bridging nickel nanoparticles, (B) a characteristic cauliflower structure, and (C, D) the branched nature of CNT with dendritic nickel growth.

According to the friction coefficient results shown in Table 2, the composite coating with the addition of CNT initially shows improved performance in reducing friction and anti-wear properties. However, as the concentration of CNT increases to 1.5 g/L, the friction coefficient of the coating surface increases. Based on the excellent intrinsic mechanical properties of GO and CNT, GO and CNT are separated from the surface of the composite coating. When the amount of CNT is 0.5 g/L, a much smaller amount of CNT is deposited on the coating. By forming a GO layer on the friction pair surface, the friction pairs do not have direct contact with each other.

In addition, high-strength CNT, due to their scaffold structure, can create rolling friction instead of sliding friction; in other words, they can play supportive role and reduce the coefficient of friction. In contrast, Composite coatings with increasing the concentration of CNT (1.5 g/L), cause CNT to agglomerate on the coating surface, which negatively affects the tribological properties by causing defects and facilitating delamination during the friction process. In composite coatings with a lower amount of CNT (0.5 g/L), fewer agglomerates of CNT and GO are deposited in the coating.

Table 2
Hardness, coefficient friction and weight loss of different composite coating.

Sample	Hardness (HV)	Coefficient of friction	Weigh loss (g)
Ni/0.5GO/0.5CNT	826	0.38	0.0005
Ni/0.5GO/1CNT	840	0.24	0.0002
Ni/0.5GO/1.5CNT	815	0.46	0.0008

Post-wear analysis of the composite coatings, conducted via pin-on-disk testing under dry conditions, is presented in the micrographs of Fig. 5. On all coated samples, the worn surfaces reveal grooves running parallel to the sliding direction, indicating that abrasion was the dominant wear mechanism. The worn surfaces of all coatings showed significant damage, characterized by broad areas of delamination and extensive ploughing by the pin. Table 2 shows the hardness and tribological behavior of the coated samples.

As can be seen, the hardness value first increases from 826 HV for Ni/GO/0.5 CNT to 840 HV for Ni/0.5GO/1CNT and then decreases to 815 HV for Ni/0.5GO/1.5 CNT. Due to the high toughness and inherent strength of GO and CNT, the hardness of the samples increases.

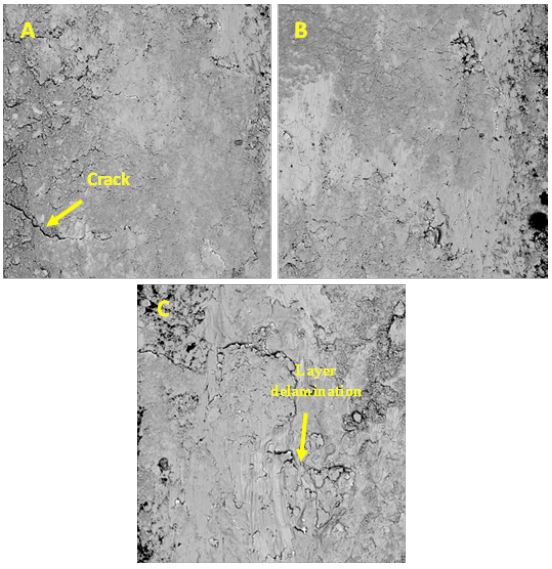

Fig. 5. SEM image of the worn surfaces of composite coating (A) Ni/0.5GO/0.5CNT (B) Ni/0.5GO/1CNT (C) Ni/0.5GO/1.5CNT.

Agglomeration of CNT and GO, caused by increasing the CNT concentration to 1.5 g/L, introduces defects such as cracks and porosity. The adhesion strength test results, displayed in Fig. 6, reveal a positive correlation between CNT content (up to 1 g/L) and GO. The optimal adhesion (5.5 MPa) is achieved with a 1 g/L CNT concentration. By adding CNT to composite coatings, a skeletal structure is formed that increases load bearing; resulting in a more compact coating. When the amount of CNT reaches 1.5 g/L, it causes cumulative precipitation in the composite coating, which leads to defects and cracks on the coating surface and reduces mechanical properties.

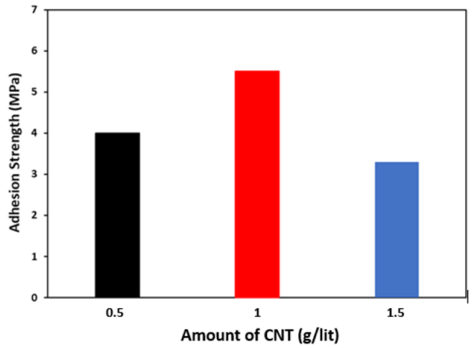

Fig. 6. Adhesion strength of the composite coatings.

4. Conclusion

This study investigated the mechanical behavior and microstructure of Ni/GO/CNT composite coatings, focusing on the effect of CNT concentration. The results demonstrate that CNTs act as effective spacers, preventing the agglomeration of GO sheets. The composite coating with 1 g/L CNT exhibited optimal properties, achieving a maximum hardness of 840 HV and a minimum wear loss of 0.0002 g. However, a further increase in CNT concentration to 1.5 g/L led to agglomeration, which reduced the hardness to 815 HV and increased the weight loss to 0.0008 g. Therefore, an optimal CNT concentration of 1 g/L is essential for maximizing the mechanical and tribological performance of the composite coating.

Author contributions

Mahdi Aghaee Malayeri: Conceptualization, Writing –original draft, Writing –review & editing; **Hassan Koohestani:** Writing – original draft, Writing –review & editing; **Mohammad Tajally:** Writing –original draft, Writing –review & editing.

Funding

No funding was received for this study.

Conflict of interest

The authors declare no conflict of interest.

Data availability

No data is available.

REFERENCES

[1] J. Freudenberger, H. Warlimont, Copper and Copper Alloys, in: H. Warlimont, W. Martienssen (Eds.), Springer Handbook of Materials Data, Springer International Publishing, Cham, 2018, pp. 297-305.
[2] C. Li, W. Huan, Y. Xuming, Special purpose equipment design of crystallizer copper tube for inner hole plating, Proceedings of the 2015 6th International Conference on Manufacturing Science and Engineering, Atlantis Press, 2015, pp. 1191-1194.
[3] O.O. Ekerenam, A.I. Ikeuba, C.N. Njoku, D.I. Njoku, W. Emori, I.K. Nwokolo, I.-I.N. Etim, B.O. Okonkwo, I.I. Udoh, E.F. Daniel, P.C. Uzoma, B.O. Awonusi, S.K. Kolawole, I.P. Etim, O.S. Olanrele, Advancements in corrosion studies and protective measures for copper and copper-based alloys in varied environmental conditions, Results in Engineering 26 (2025) 105257.
[4] M. Aghaee Malayeri, H. Koohestani, M. Tajally, Improving the properties of nickel/graphene oxide coated copper plate by changing the electroplating process conditions, Results in Engineering 18 (2023) 101167.
[5] H. Zhang, N. Zhang, F. Fang, Fabrication of high-performance nickel/graphene oxide composite coatings using ultrasonic-assisted electrodeposition, Ultrasonics Sonochemistry 62 (2020) 104858.
[6] J. Chen, J. Li, D. Xiong, Y. He, Y. Ji, Y. Qin, Preparation and tribological behavior of Ni-graphene composite coating under room temperature, Applied Surface Science 361 (2016) 49-56.
[7] H. Algul, M. Tokur, S. Ozcan, M. Uysal, T. Cetinkaya, H. Akbulut, A. Alp, The effect of graphene content and sliding speed on the wear mechanism of nickel–graphene nanocomposites, Applied Surface Science 359 (2015) 340-348.
[8] R. Askarnia, S.R. Fardi, M. Sobhani, H. Staji, H. Aghamohammadi, Effect of graphene oxide on properties of AZ91 magnesium alloys coating developed by micro-arc oxidation process, Journal of Alloys and Compounds 892 (2022) 162106.
[9] S.R. Fardi, H. khorsand, R. Askarnia, R. Pardehkhorram, E. Adabifiroozjaei, Improvement of biomedical functionality of titanium by ultrasound-assisted electrophoretic deposition of hydroxyapatite-graphene oxide nanocomposites, Ceramics International 46(11, Part A) (2020) 18297-18307.
[10] A. Bahri, R. Askarnia, J. Esmaeilzadeh, S.R. Fardi, Mechanical and electrochemical behaviors assessments of Aluminum-Graphene Oxide composites fabricated by mechanical milling and repetitive upsetting extrusion, Journal of Composites and Compounds 3(8) (2021) 152-158.
[11] V.T. Dang, D.D. Nguyen, T.T. Cao, P.H. Le, D.L. Tran, N.M. Phan, V.C. Nguyen, Recent trends in preparation and application of carbon nanotube–graphene hybrid thin films, Advances in Natural Sciences: Nanoscience and Nanotechnology 7(3) (2016) 033002.
[12] S.-D. Seo, I.-S. Hwang, S.-H. Lee, H.-W. Shim, D.-W. Kim, 1D/2D carbon nanotube/graphene nanosheet composite anodes fabricated using electrophoretic assembly, Ceramics International 38(4) (2012) 3017-3021.
[13] F. Gutiérrez-Mora, R. Cano-Crespo, A. Rincón, R. Moreno, A. Domínguez-Rodríguez, Friction and wear behavior of alumina-based graphene and CNFs composites, Journal of the European Ceramic Society 37(12) (2017) 3805-3812.
[14] S. Khabazian, S. Sanjabi, The effect of multi-walled carbon nanotube pretreatments on the electrodeposition of Ni–MWCNTs coatings, Applied Surface Science 257(13) (2011) 5850-5856.
[15] N.B. Hoveizavi, M. Laghaei, S. Tavakoli, B. Javanmardi, Wearable biosensors incorporating nanocomposites: advancements, applications, and future directions, Journal of Composites and Compounds 6(21) (2024).
[16] P. Yang, Y. Chen, J. Zhang, B. Shu, Electrochemical co-deposition of carbon nanotube/Ni composite layer, Materials Chemistry and Physics 308 (2023) 128284.
[17] Y.-r. Dong, W.-c. Sun, X.-j. Liu, Z.-w. Jia, F. Guo, M. Ma, Y.-y. Ruan, Effect of CNTs concentration on the microstructure and friction behavior of Ni-GO-CNTs composite coatings, Surface and Coatings Technology 359 (2019) 141-149.
[18] A.A. Javidparvar, R. Naderi, B. Ramezanzadeh, Epoxy-polyamide nanocomposite coating with graphene oxide as cerium nanocontainer generating effective dual active/barrier corrosion protection, Composites Part B: Engineering 172 (2019) 363-375.
[19] Q.-l. Rao, G. Bi, Q.-h. Lu, H.-w. Wang, X.-l. Fan, Microstructure evolution of electroless Ni-B film during its depositing process, Applied Surface Science 240(1) (2005) 28-33.